

STUDIES ON THE CONVERSION OF A RIVER CARGO BARGE INTO A FLOATING FISH FARM

Costel UNGUREANU, Adrian PRESURĂ, Radu BOSOANCĂ, Andreea MÂNDRU, Silviu PERIJOC, Victor MIHAI, George COTOC
"Dunarea de Jos" University of Galati, Naval Architecture Faculty, Romania
e-mail: costel.ungureanu@ugal.ro

ABSTRACT

This paper presents results of the research and developing of a modular floating aquaculture platform based on inland river cargo barge design to be exploited under biosecurity and sustainability conditions in the Lower Danube region, aligned with the current sustainable development strategies of the blue economy outlined by the European Union. The new design combines the capabilities of growing fish in modular tanks with the growing vegetables in recirculating systems in the greenhouse superstructure of the floating platform. The first step of this interdisciplinary and multidisciplinary research is a full naval architecture study, meaning both aerodynamically and strength calculation, as a starting point for the design and evaluation of the growing fish and cultivating vegetables systems.

KEYWORDS: fish farm, aquaculture platform, river barge, CFD, FEM, wind tunnel

1. Introduction

In 2019 the construction of the world's first 100,000-tonne large-scale fish farming ship started in China, pioneering a new mode of industrial farming with "movable fish farms" on distant seas [1]. The Conson Group plans to invest in the construction of an aquaculture armada consisting of 50 such ships with a gross tonnage of 100,000 tons each, which are expected to annually produce about 200,000 tons of seawater fish with an annual output value exceeding 11 billion yuan (\$1.68 billion). With a length of 249.9 meters, a width of 45 meters, and a designed speed of 10 knots, the vessel can avoid typhoons, red tides and other severe weather and disasters, conducting aquaculture operations in seas around the world.

Culturing tests were conducted from May to August 2021 on a test aquaculture vessel in the sea regions of Zhejiang, China [2]. The growth rate of *Pseudosciaena crocea* reaches 100 g per month, and the survival rate gets to 95 %, which proves the feasibility of the Shipborne mariculture system.

Recently, a semi-submersible vessel-shaped fish farm platform was proposed [3] Pang *et al.* (2023). By diving its main body through the water its seakeeping performance under extreme conditions improved. Therefore, the small waterplane area

provided a reference for the design of a large fish farm platform.

Chu *et al.* performed a comprehensive review on the existing design guidelines and technical guidance from maritime classification rules/standards and national and inter-national standards with applicability to offshore fish farming installations with direct interest to aquaculture engineers and designers when developing offshore fish farming infrastructure [4].

The aquaculture industry is aiming to move fish farms from nearshore areas to open seas because of many attractive advantages in the open water [5]. However, the major challenge is to design the structure to withstand the harsh environmental loads due to wind, waves, and currents. Contrary to maritime fish farms, the inland rivers and channels offers to fish farms, either moored or anchored, a more protected area. In this case the wave loads are negligible and in the case of farms with large superstructures the influence of the wind loads must be investigated.

This paper presents the results of the research on the conversion of a cargo river barge into a floating fish farm, for the inland rivers in the Lower Danube region of Romania. The study is developed based on the following objectives:

- Analysis of existing floating fish farms and definition of parameters and conditions for the design of the floating structure
- General arrangement of the barge as a floating fish farm
- Numerical investigations of barge strength using FEM
- Numerical investigations of barge superstructure aerodynamic characteristics using CFD
- Wind tunnel investigations of barge superstructure aerodynamic characteristics using EFD.

2. Fish farm design

The 3000 tons typical barge was considered as base for the conversion into a fish farm for which the main dimensions are presented in Table 1. As can be seen in Figure 1 a greenhouse was considered above the main deck, covering fish tanks and aquaponics systems, and the cargo hull was separated into 12 modular tanks. At midship a pump room was considered below main deck, and a technological container was placed above.

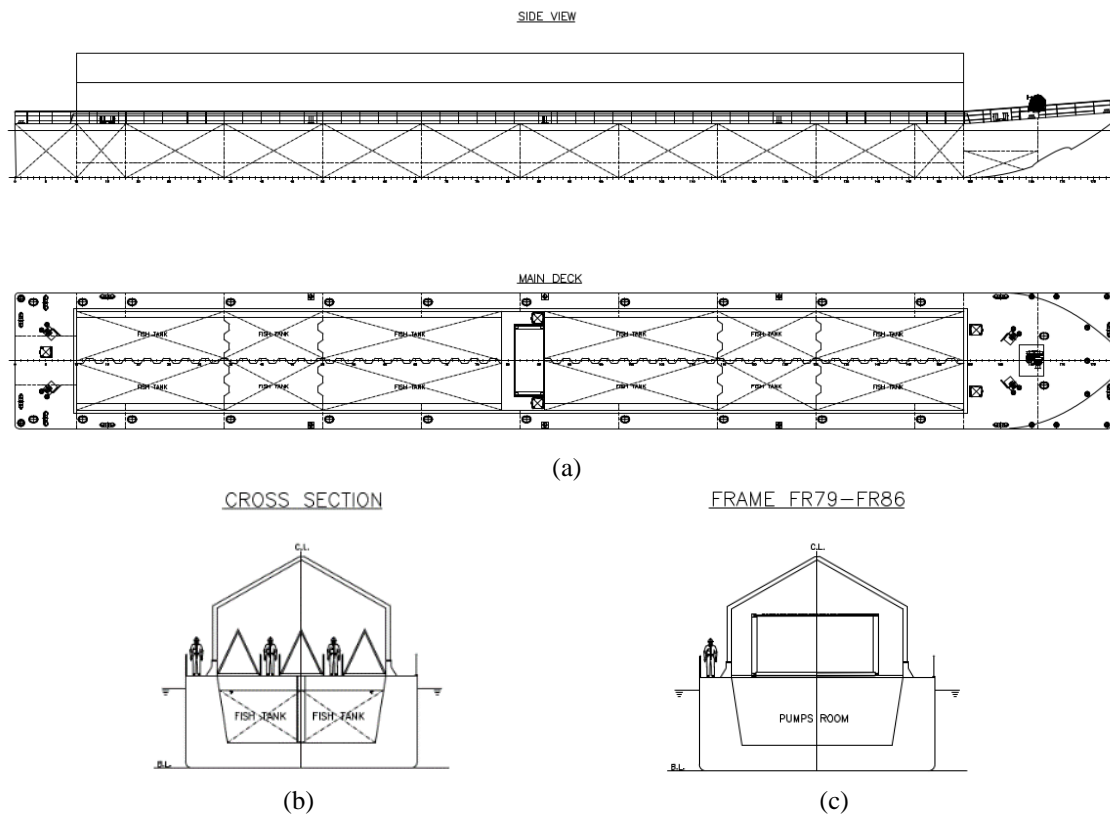


Fig. 1. General arrangement of the fish farm: (a) Side and top view; (b) Transversal view -typical section, (c) Transverse section at midship

Table 1. Barge main dimensions

Main dimensions	Value	Units
Length overall	89.0	meters
Height overall	10.5	
Beam	11.0	meters
Depth	4.4	meters
Draught	3.8	meters
Bloc coefficient	0.935	-
Displacement	3459	tons

As stated before, solar panels can be mounted either above fish tanks, providing direct sun protection to fish water, or to greenhouse top

providing both electrical energy and shade to plant growing systems. The latter was considered in the present research. Knowing that the average tilt angle

of photovoltaic panels during warm months was found to be approximately 29° [6] in an area close to the main target area of this project, lead to a 30°

inclination design angle for the greenhouse roof. In Figure 2 the proposed conceptual design is presented.



Fig. 2. The fish farm concept: (a) Fore starboard view; (b) Greenhouse interior view

Based on the proposed design a numerical strength verification is performed to assess the loading capacity of fish farm. After that, an aerodynamical, both numerically and experimentally, investigation is performed from floating establishment naval architecture point of view.

3. Strength verification

Performing a 3D-FEM (Finite Element Method) analysis on extended FE models has become nowadays relatively accessible, allowing more improvements to be included in a single design step, resulting in a final product that meets the safety criteria over its entire life cycle [7]. The slender body of the barge, combined with a large main deck opening and a shallow draught result in a low bending and torsional rigidity. The sum of the above facts can lead to local failure and loss of structural integrity if

stress levels are not evaluated properly in the design stage [8]. Since the structure of typical inland barge is subjected throughout its life cycle to structural changes due to minor collisions, either ship-to-ship or ship-to-quay, shallow-water groundings, corrosion, fatigue, the strength, and stability of the barge structure can be drastically reduced [9]. This part is aiming to investigate 3D-FEM global structural analysis of an inland barge retrofitted as floating fish farm considering the still water condition and full load condition based on the equivalent quasi-static approach [10-12].

A surface 3D-CAD model of the barge with greenhouse was generated using the Ansys built-in modeler Space Claim (Figure 2). The steel grade A material formulation with yield stress limit of 235 MPa and rupture stress limit of around 400 MPa is provided.

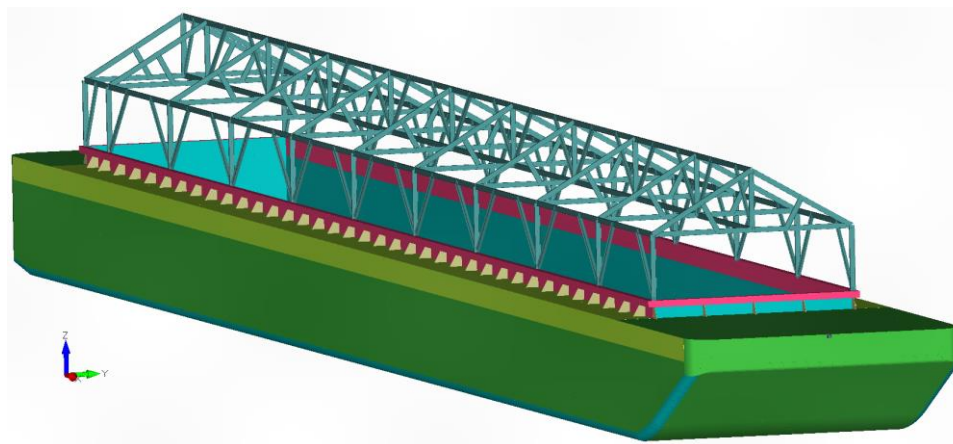


Fig. 2. CAD model of barge with greenhouse

Next, the results obtained following the analysis of the 3D-FEM model for the river barge in full loading condition are presented. The loading cases sets are as following:

- LC_1 - Still water condition;
- LC_2 - Full loading condition -hogging;
- LC_3 - Full loading condition - sagging.

Hydrostatic pressure on the outside shell and on inner hull was applied and together with the numerical results for the LC1 is presented in Figure 3.

The fish farm was designed to be anchored or moored to quay, but waves generated by the shipping on rivers and channels may reach the local position.

Therefore, a study for the evaluation of stress assessment in respect to wave loads was performed for both cases hogging and sagging. The numerical results are plotted as deformed view in Figure 4. The wave height for was considered 1.2 m.

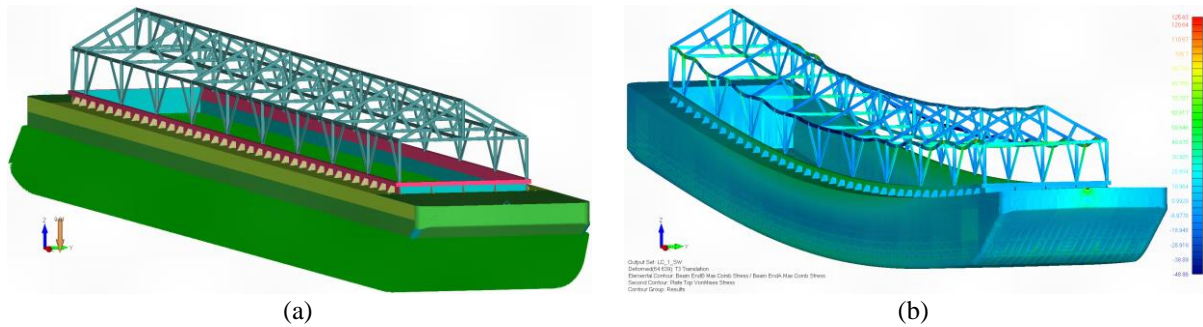


Fig. 3. LC1-Still water condition:(a) Model with applied hydrostatic pressure, (b)FEM results, deformed view

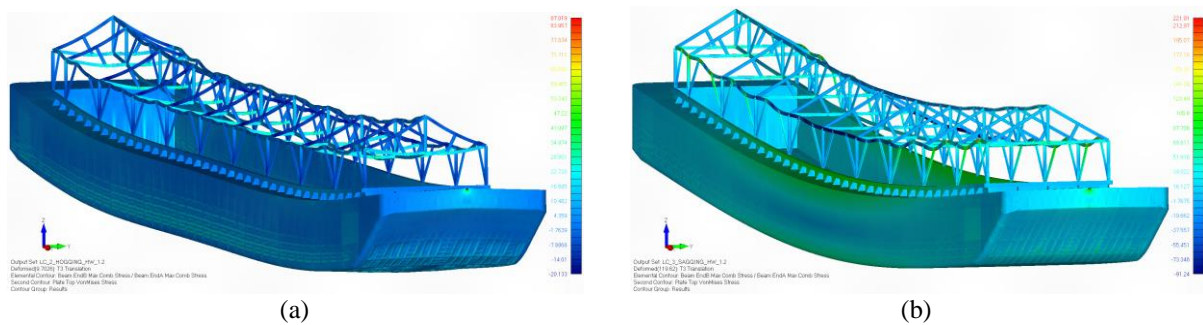


Fig. 4. Von Mises stress, deformed view: (a) LC2-Hogging, (b) LC3-Sagging

It was observed that the maximum Von Mises stress obtained was 125 MPa for the still water case, 87 MPa for hogging case and 222 MPa for sagging case.

The current study presents a global structural 3D-FEM analysis of a typical open-top, double-hull barge, having a cargo capacity of 3000 dwt with a greenhouse superstructure. In the framework of analysis and data interpreting processes it can be concluded that the current structural layout of the barge does not present any structural risk. The FE results examination pointed out some structural hot-spots, especially for LC3 case where yielding ratio found to be higher than 0.8, that require updates for a better distribution of the local occurring stresses. Further investigations must be performed after the structural update of the identified hot-spot areas, completed by other strength criteria.

4. Aerodynamic investigations

Two types of methods are known for the study of aerodynamic flow around the barge as fish farm

with greenhouse mounted on main deck: experimental and numerical. Experimental investigation involves complex research infrastructure, such as wind tunnels and measuring equipment. The experiments provide a quantitative description of the flow measurements individually for each investigated physical quantity, in a limited number of points in the flow field for a small range of problems and experimental conditions. Experiments are also expensive, slow, sequential, and repetitive. Another important element in experimental research is model manufacturing. So, in this research, the experimental study on the model is used only for the validation of the global aerodynamic performances of the new concepts.

4.1. Experimental investigations

The experiments were carried out in the Wind tunnel of the Naval Architecture Faculty, “Dunarea de Jos” University of Galati, presented in Figure 5a, [13]. The main dimensions of the wind tunnel are length = 17 m, width = 3.7 m and height = 3.4 m.

Also, the main dimensions of the measuring section of the tunnel are length = 2.5 m, width = 0.82 m and height = 0.58 m. The maximum air velocity of 23.5 m/s can be obtained, and the maximum physical model length of 2 m can be used in the wind tunnel. The wind tunnel drive system includes an axial flow blower with variable speed and a motor power of 55 kW and 1450 RPM.

Using a 3D printer, the experimental model presented in Figure 5b was printed at a scale of 1:150, having the following main dimensions, where m is for model: $L_m = 600$ mm, $B_m = 73$ mm, Air draft surface model $2.58222 \times 10^{-3} \text{ m}^2$. Only the upper part of the model containing the new superstructure and all exposed surfaces to wind loads was tested.

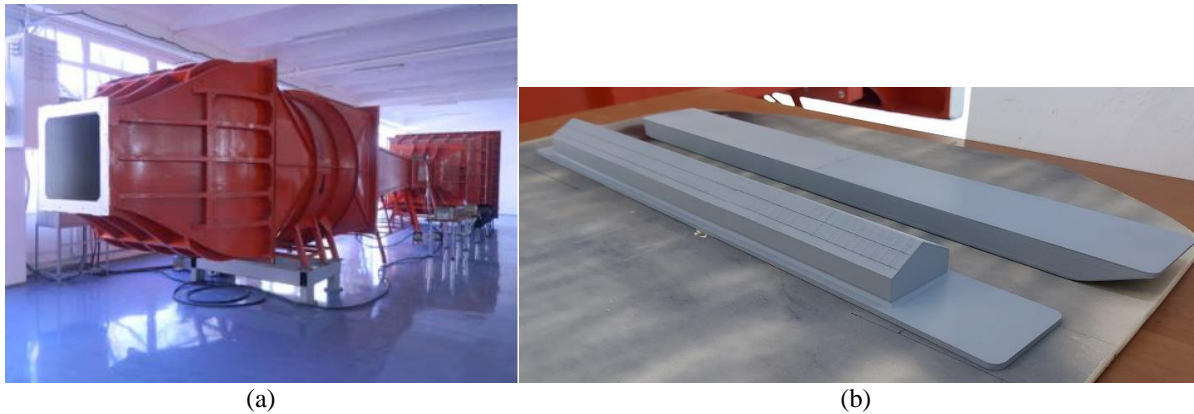


Fig. 5. Wind tunnel: (a) Global view; (b) Experimental model

For this experimental model, specific equipment was used to be able to accurately measure the air velocity and the forces and moments that apply on the model. For this reason, a highly accurate Pitot tube was used conned to a 16-channel pressure scanner, which was used to measure differential pressure (dynamic pressure) in the measuring section. The scanner has its own software for measuring the analogical data and changing it to digital data to calculate air velocity. Once knowing the dynamic pressure (P_{dyn}) value, the air velocity (v) can be extracted from the following formula:

$$P_{dyn} = 0.5 \rho v^2 \quad (1)$$

where density (ρ) varies with the air temperature inside the testing facility.

The air temperature throughout the day of testing was 20° C and consequently the air density, used in the calculation for the air velocity, was 1.025 kg/m³.

In Figure 6, the results for longitudinal, F_x , and lateral, F_y , drag force components are presented in respect of angle of attack.

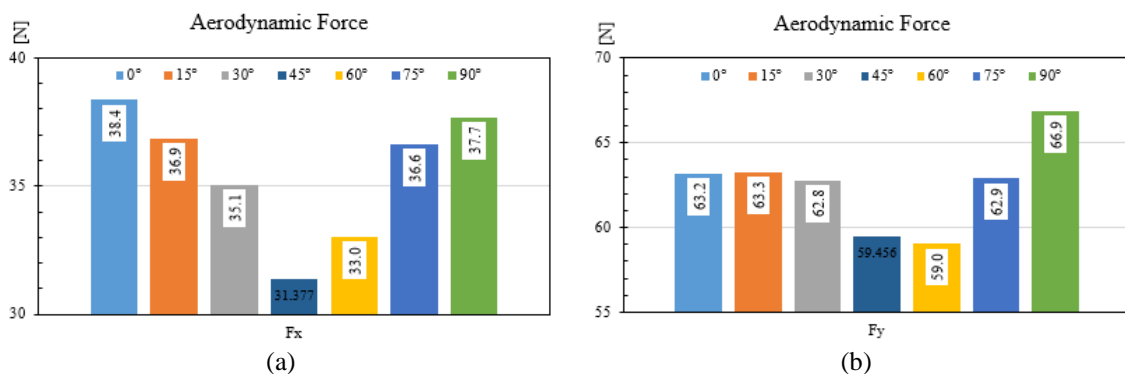


Fig. 6. Measured aerodynamic forces diagrams (a) F_x ; (b) F_y

4.2. Numerical investigations

The alternative to experimental investigations is numerical simulations (CFD-computational Fluid

Dynamics), which have gained significant popularity, especially after the development of advanced numerical methods and the advent of digital machines with high computing power. In general, numerical

simulations offer a wide range of advantages over similar experimental research. First, numerical simulations provide a quantitative prediction of the flow simultaneously for all investigated physical quantities, in a very large number of points in time and space. Second, a numerical solution substantially reduces design and production times and costs. At the same time consumed by a case, as many cases can be studied as there are computing machines available.

In this study, the governing equations were solved using the Reynolds-Averaged Navier-Stokes (RANS) method. The commercial CFD code NUMECA/FineMarine, was used to solve these mass and momentum conservation equations. In the Cartesian coordinate system, the averaged continuity and momentum equations for incompressible flows, including external forces (2 and 3), can be expressed in tensor form as:

$$\frac{\partial(\rho \bar{u}_i)}{\partial x_i} = 0 \quad (2)$$

$$\frac{\partial(\rho \bar{u}_i)}{\partial t} + \frac{\partial}{\partial x_j} (\rho \bar{u}_i \bar{u}_j + \rho \overline{u'_i u'_j}) = -\frac{\partial \bar{p}}{\partial x_i} + \frac{\partial \bar{\tau}_{ij}}{\partial x_j} \quad (3)$$

where ρ is density, u_i is the relative averaged velocity vector of flow between the fluid and the control volume, $u'_i u'_j$ is the Reynolds stresses, \bar{p} is the mean pressure, and τ_{ij} is the mean viscous stress tensor component for Newtonian fluid under the incompressible flow assumption, and it can be written as in equation 4:

$$\bar{\tau}_{ij} = \mu \left(\frac{\partial \bar{u}_i}{\partial x_j} + \frac{\partial \bar{u}_j}{\partial x_i} \right) \quad (4)$$

in which μ is the dynamic viscosity.

To solve the incompressible steady RANSE in a global approach, the solver uses the finite volume method to generate the spatial discretization for the governing equations [14]. The RANSE's convection and diffusion terms are discretized using a second-order upwind scheme and a central difference scheme. The velocity field is calculated using

momentum conservation equations, while the pressure field is determined using the mass conservation constraint, which is then transformed into a pressure equation. Additional transport equations for modelled variables are discretized and solved in the case of turbulent flows using the same principles, as described by [15]. In this study, the k- ω SST turbulence model with wall function formulation and wall roughness model implemented is employed for turbulence closure.

Being designed as a floating establishment, the fish farm is associated with a land construction and the wind velocity value is calculated based on the imposed dynamic pressure which in the subject area is equal to 0.6 [16]. Also, multiple wind direction was taken into consideration, as can be seen in Figure 6 (a), for one side covering of 180° with a step of 15°. The other side is considered symmetrical, and it was not investigated.

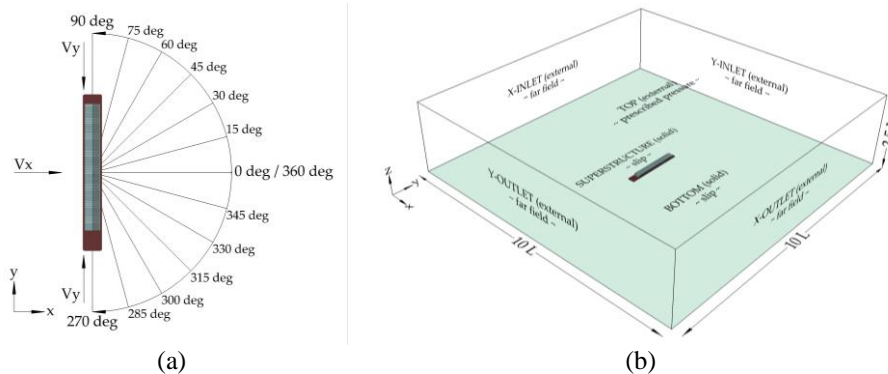


Fig. 6. Numerical model: (a) Angle map of wind directions in respect to barge; (b) Computational domain with boundary conditions

To avoid the reflection of the wind from the lateral boundaries, producing numerical instabilities a box type computational domain was generated with

10 x 10 x 2.5 L dimensions. The boundary conditions, shown in Figure 6 (b), have been chosen to be compatible with the numerical wind tunnel principle

calculation, namely farfield with the imposition of the velocity. The solid wall condition was imposed on the model and on the bottom boundary to simulate the flow inside wind tunnel.

An unstructured hexahedral mesh has been generated to cover the entire computational domain along the barge model. The grid topology is an H-H type. Details of the near-hull corner grids and on the hull, itself are presented in Figure 7.

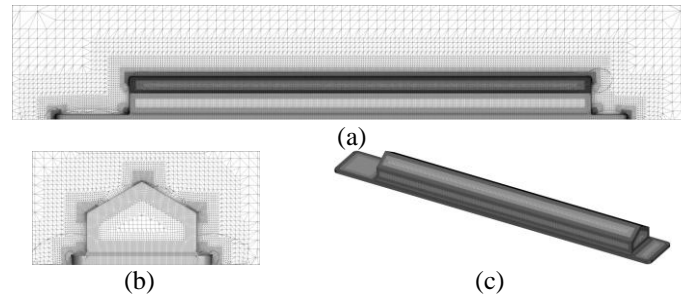


Fig. 7. Numerical grid: (a) Longitudinal section; (b) Transverse section; (c) Gridlines on barge model

Next, the results for full scale numerical investigations are presented. The pressure effect of wind on a greenhouse can have significant implications for its structural integrity and the well-being of the plants inside. Wind creates both positive and negative pressure on the surfaces of the greenhouse. Positive Pressure: Wind hitting the windward side of the greenhouse creates positive pressure. It pushes against the structure, potentially causing stress on the materials, joints, and supports. Negative Pressure: On the leeward side or the sides where the wind flows around, it creates a negative pressure zone. This can cause suction forces that may try to pull the structure outward. These pressure

effects can vary based on factors such as wind speed, direction, the design of the greenhouse, its orientation to prevailing winds, and the materials used in its construction. Aligning the greenhouse in a direction that minimizes exposure to prevailing winds can reduce direct impact. This is possible on lakes or open seas where the fish farm can be anchored and can easily rotate to be properly aligned with the wind direction. For rivers and channels the available space for manoeuvring is limited. Therefore, the pressure and the turbulence on the greenhouse are computed and presented next. The pressure is presented for both sides positive and negative in Figure 8.

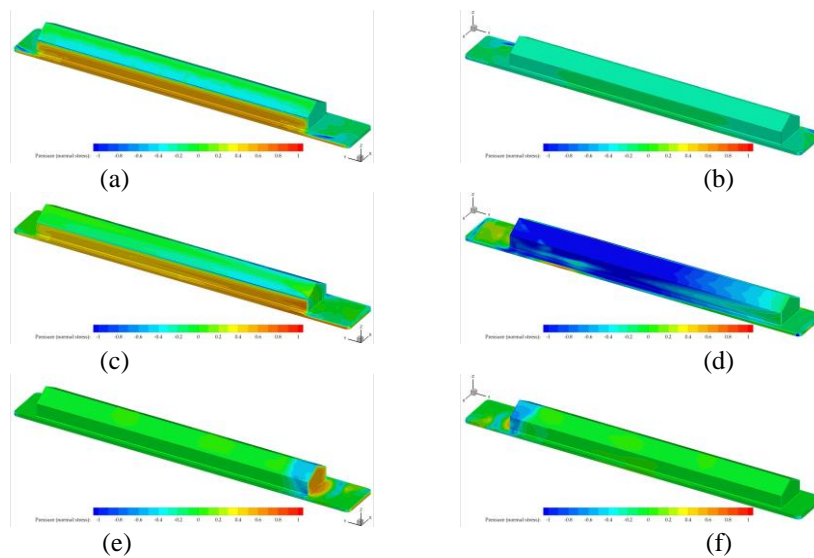


Fig. 8. Pressure distribution on greenhouse and on hull above free surface: (a) 0° - positive side, (b) 0° - negative side, (c) 45° - positive side, (d) 45° - negative side, (e) 90° - positive side, (f) 90° - negative side

Turbulence caused by wind loads on a greenhouse can create complex airflow patterns that affect the structure and the plants within it. Wind turbulence is characterized by irregular fluctuations in wind speed and direction. Turbulence creates varying pressure points on different parts of the greenhouse. This can lead to uneven stress distribution across the structure, potentially causing weak points or areas

prone to damage. Understanding the potential effects of turbulence and taking proactive measures during the design, construction, and maintenance of the greenhouse can help minimize its negative impact on the structure and the plants grown within it. Next, Figure 9 presents the turbulence evolution in respect to wind direction.

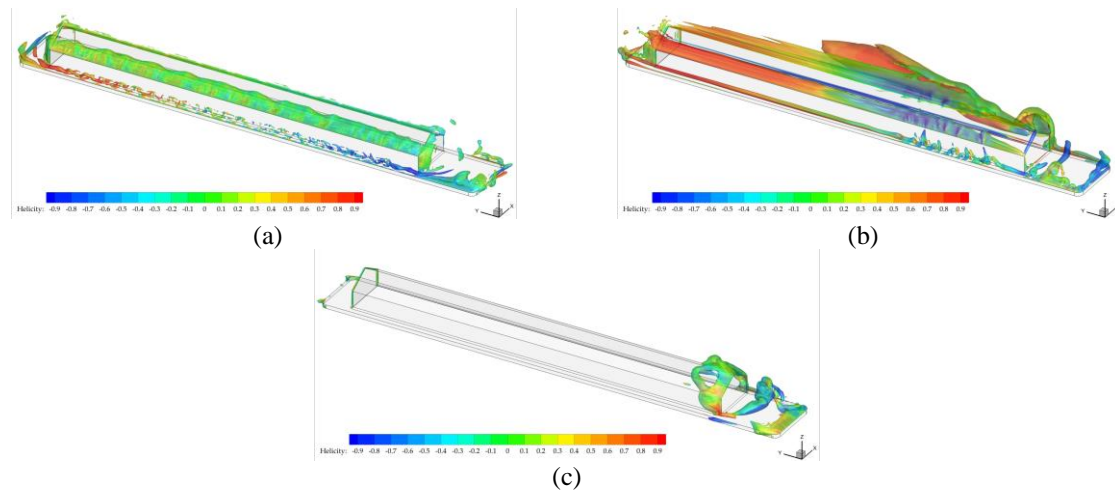


Fig. 9. The turbulence evolution in respect to wind direction

5. Conclusions

This research proposed for the first part of this interdisciplinary and multidisciplinary research a conversion from a cargo river barge to a modular floating fish farm. Before evaluating the fish and vegetables cultivation systems a full naval architecture study, meaning both aerodynamic and strength calculation, was performed.

The novelty of this study is the realization of a pilot project of a modular aquaculture platform for exploitation under biosecurity and sustainability conditions in the Lower Danube region, aligned with the current sustainable development strategies of the blue economy outlined by the European Union.

Acknowledgement

This project was financed through the financing program for Sustaining and developing research activities CDI-TT of „Dunarea de Jos” University of Galati, Contract no. 9416/30.03.2023. All studies were performed using the research facilities of the Naval Architecture Faculty and of the Naval Architecture Research Center, such as the numerical hydrodynamics laboratory, the numerical structural analysis laboratory, the wind tunnel, as well as the integrated design systems for hull and ship systems.

References

- [1]. Times G., *Construction begins on world as first 100,000 farming vessels in Qingdao*, <https://www.globaltimes.cn/content/1210431.shtml>, 2020.
- [2]. Zhisong L., Xiaoyu G., Mingchao Cui., *Numerical investigation of flow characteristics in a rearing tank aboard an aquaculture vessel*, *Aquacultural Engineering*, vol. 98, 102272, <https://doi.org/10.1016/j.aquaeng.2022.102272>, August 2022.
- [3]. Pang G., Zhang S., Liu H., Zhu S., Yuan T., Li G., Han X., Huang X., *Hydrodynamic response analysis for a new semi-submersible vessel-shaped fish farm platform based on numerical simulation*, *Front. Mar. Sci.*, 10:1135757. doi: 10.3389/fmars.2023.1135757, 2023.
- [4]. Chu Y. I., Wang C. M., Zhang H., Abdussamie N., Karampour H., Jeng D. S., Baumeister J., Aland P. A., *Offshore Fish Farms: A Review of Standards and Guidelines for Design and Analysis*, *J. Mar. Sci. Eng.*, 11, 762. <https://doi.org/10.3390/jmse11040762>, 2023.
- [5]. Li L., Jiang Z., Høiland A., Ong M., *Numerical Analysis of a Vessel-Shaped Offshore Fish Farm*, *Journal of Offshore Mechanics and Arctic Engineering*, 140. 041201. 10.1115/1.4039131, 2018.
- [6]. Manolache A. I., Andrei G., Rusu L., *An Evaluation of the Efficiency of the Floating Solar Panels in the Western Black Sea and the Razim-Sinoe Lagunar System*, *J. Mar. Sci. Eng.*, 11, 203. <https://doi.org/10.3390/jmse11010203>, 2023.
- [7]. Domnisoru L., *Numerical approach for global ship strength analysis based in 1D-Beam model, under oblique equivalent quasi-static wave loads*, Galati University Press: Shipbuilding, 38, p. 27-36, 2015.
- [8]. Savin M., Presura A., Chirica I., *Environmental protection using structural analysis of ships*, *Sea Conf. IOP Conference Series: Journal of Physics (1297)*, Article 012015, 2019.



- [9]. **Meinken A., Schlüter H. J.**, *Collapse behavior of a push-barge*, Marine Structures, 15(2), p. 193-209, 2002.
- [10]. **Domnisoru L.**, *Special chapters on ship's structures analysis*, Applications (Galati: The University Foundation „Dunarea de Jos” Publishing House), 2017.
- [11]. **Domnisoru L.**, *Strength assessment in oblique design waves for a Europe B2 1740T river barge type*, Galati University Press: Shipbuilding, 41, p. 23-28, 2019.
- [12]. **Domnisoru L.**, *On the strength assessment of a small liquid petroleum gas carrier in oblique waves by 1D and 3D-FEM analyses*, ModTech. IOP Conference Series: Materials Science and Engineering, (916) Article 012027, 2020.
- [13]. **Obreja D.**, *Experimental Techniques in the Wind Tunnel of Naval Architecture Faculty*, Annals of "Dunarea de Jos" University Galati. Fascicle XI, Shipbuilding, 2021.
- [14]. **Guilmineau E., Deng G. B., Leroyer A., Queutey P., Visonneau M., Wackers J.**, *Influence of the turbulence closures for the wake prediction of a marine propeller*, Proc. of the 4th International Symposium on Marine Propulsors, 2015.
- [15]. **Duvigneau R., Visonneau M., Deng G. B.**, *On the role played by turbulence closures in hull shape optimization at model and full-scale*, Journal of Marine Science and Technology, 8 (1) p. 1-25, 2003.
- [16]. ***, CR 1-1-4/2012. Cod de proiectare, *Evaluarea actiunii vantului asupra constructiilor*.